Memoirs of the Faculty of Engineering, Nagoya University
Vol. 30 No. 2. (1978)

THEORETICAL APPROACH TO THE SWITCHING ARC PHENOMENA IN ELECTRIC POWER SYSTEMS

IWAO MIYACHI

Department of Electrical Engineering

(Received November 8, 1978)

Abstract

The physical properties and electric characteristics of the arc commonly found in switching operation of power systems are discussed in detail by introducting the fundamental constants of high temperature gases such as air and SF_6. Temperature profiles inside the arc column are theoretically deduced for given current intensity and thermal arc radius with experimental confirmation. The effects of the electrode-metal vapour evaporated inside the column and the radiation energy from the arc core are also studied theoretically. The voltage gradient against current characteristics of the arc are decided by analytical method at first and by numerical calculation later more precisely from the electrical point of view. The time constant of arc conductance and the high temperature breakdown voltage are fully analysed based on the newly introduced theoretical consideration. The application of spiral arc is also proposed as a suitable device for direct current interrution. Then, some of the topics among the engineering requirements now being considered in the world-wide research and development of circuit-breakers in electric power systems are discussed from the viewpoints of restriking voltage, interrupting process and verification of capability. Finally, those requirements are surveyed with the above-mentioned detailed knowledge of fundamental concepts on physical properties and electric characteristics of switching arc.

CONTENTS

1. Preface

The harmonized combination of science and engineering is really considered to be necessary to the economical development of modern industrial technolgy. In this case, when one makes a decision to set up a research program, an actual problem occurs by which direction this conformity should have to be taken place. So many parameters of an individual case are likely to disturb the proof test procedure on the one hand, and an extremely simplified theoretical model does not represent the actual properties on the other. In this point of view, the author has had the opinion that the best way to develop the engineering science problem should have the direction from science to engineering sustained by fully experienced technological common sense preferably directed by a research engineer. Also, the process might be carried out rather theoretically, say 70%, than experimentally to expect the wide range application of the result obtained to the highest possible extent. This report contains some of the items studied by the author and his collaborators with the fifteen years' experience for switching overvoltages and another fifteen years' for arc physics. The research program set up ten years ago is still valid at present for the sake of the continuous execution of the schedule.

The study on the arcing phenomena is a time-honoured special article which necessitates always the drastic knowledge based on progressive understanding. The electric power systems all over the world directly relate to the high-power electric arc through the equipment such as EHV and UHV circuit-breakers and lightning arresters as well as the short-circuit fault current. The natural thunderbolt, which threatens the electrical installations and eventually the human life, is also a sort of arc discharges. This paper deals with the arcing phenomena from physical and energetic points of view so as to recognize the fundamental knowledge about the matter which, in turn, will facilitates the ordinary engineering processes of design, manufacture, operation and maintenance etc.

2. Introduction

The first step to the research program for the switching arc phenomena in

power systems is to establish a bird's-eye view of the correlation between the scientific and technical terms concerned. The tentative preparation of the diagram indicating the related characteristics of the electric arc is convenient to solve the problem systematically. Those are divided into some distinct categories such as electrical properties, thermal and high temperature properties, optical properties, gaseous characteristics, electrode phenomena and pressure effect.

As the arc is burning at a high temperature of some tens of thousand degrees with the temperature gradient inside surrounded by the stabilizing wall or the non-conductive gaseous stream, it must be analysed from purely thermodynamic point of view even in its steady state condition. The shape of the ordinary switching arc is relatively long with small cross sectional area and the electric energy produced shall be dissipated radially through the outer surface of the arc column. The sum of the voltage gradient along the column together with the instantaneous anode and cathode drops determine the total arc voltage between the electrodes. This is why the author is devoted to compile the theoretical data on the voltage gradient against current with the consideration of the high temperature properties of different sort of gaseous mixture under a given surrounding pressure.

Optical diagnostics are most convenient measures to analyse the constituent particale densities of an arc. According to the condition of local thermal equilibrium (LTE) considered, a series of the thermal dissociation of gas molecules followed by the excitation and the multiple ionizations of atoms is taking place with the balanced reverse processes. The characterized spectral lines and continuum will show exactly what is going on inside the luminous part of the arc column. All sorts of gases are likely to be electrically conductive at a high temperature above 4500 degrees Kelvin and naturally in the lower temperature range they are non-conductive with their own different insulation strength corresponding to the temperature. The principle of the emission of radiation for each species of transition phenomena is effectively applied to analyse the arc characterisitics. Conventional means of photography such as high speed cameras, Schlieren analysers and interferometers are also available to observe the arc profile concerning the thermal conditions of the non-luminous outer flame.

The electrode materials are occasionally predominant in the vicinity of cathode extremity. The metal vapour released is generally the atomic, excited and ionized states of copper in most cases of switching arc. The relatively low value of ionization potential of copper vapour will affect considerably the conductivity of the contaminated gas mixture. This is one of the most impotant problems in actual switching devices.

Theoretical considerations of the arc go back to those of Cassie (1939) and Mayr (1943), and they are still now utilized to a great extent with necessary modifications. The former assumes the arc channel of constant temperature with varying diameter according to the current intensity, and the latter is considering the different temperature gradient inside the column of a definite diameter. The concept of the time constants derived from those theories will not be sufficient if one wishes to have a detailed physical meaning of an arc. The author has made up a plan to establish the method of obtaining the time constant of the transient arc from the purely thermal properties of the constituent atoms and molecules. The results thus obtained are shown in this paper with the comparison of theoretical and exprimental values for an example.

The degradation of the insulation strength of gases at an extremely high

temperature is well known qualitatively but is not so clearly understood quantitatively because of the lack of the data investigated. The current interruption will be completed by the permanent restoration of the insultation strength just after the instant of current zero where the high temperature gas of about several thousands of degrees is withstanding the severe rate of rise of restriking voltage. The high temperature breakdown characteristics of air and common gases have been theoretically investigated here and the results are confirmed by experiments up to 1400 ℃.

Direct current interruption is another concern in the future transmission systems to secure the multi-terminal network against the fault. There are some proposals to construct a DC circuit-breaker so far, but any type of practical equipment is not yet utilized. The author's idea to elongate the arc length most effectively within a restricted volume of extiguishing chamber is realized by magnetically driven spiral arc with special consideration of electrode configuration. At the same time, the behaviour of running arc between two adjacent parallel conductors is also investigated. The experimental results of spiral arc will contribute to have a profound knowledge of not only the extinguishing arc characteristics but also the dynamic features of magnetically driven arc.

Those theoretical and partly experimental results mentioned above must be examined from the viewpoints of engineering requirements suitable for switching arc phenomena in electric power transmssion systems. The detailed items have been actively discussed within groups of "Gas Discharges" sponsored by Institution of Electrical Engineers (U. K.) and "Study Committee No. 13" of CIGRE (France) for the last ten years.

3. Voltage against Current Characteristics

Voltage gradient along the axis of an arc column is, at first, studied by analytical method and the process is replaced, later on, by numerical calculation. As the total electric power P_a consumed per unit length of an arc column will be dissipated radially through the outer cylindrical surface of the conducting region, say $2\pi r_c$, at temperature T_σ, the energy balance equation in unit time of steady state condition is expressed as follows,[11)13)]

$$\sigma E^2+\frac{1}{r}\frac{d}{dr}\left(r\frac{dS}{dr}\right)=0 \tag{1}$$

together with the equations

$$S(T)=\int_0^T \kappa(T)dT \tag{2}$$

$$P_a=-2\pi r_c\left[\kappa\frac{dT}{dr}\right]_{r=r_c}=-2\pi C_0 \tag{3}$$

where σ and κ are electrical and thermal conductivities with respect to temperature T and radius r. The heat transfer function S is chosen so as to carry out the

integration easily. The voltage gradient E may be calculated by solving these equations analytically. For SF_6 gas of 1 atm, σ, κ and S are approximately denoted by the following simplified equations above threshold temperature $T_\sigma=5500$ K as shown in Figs. 1 and 2.

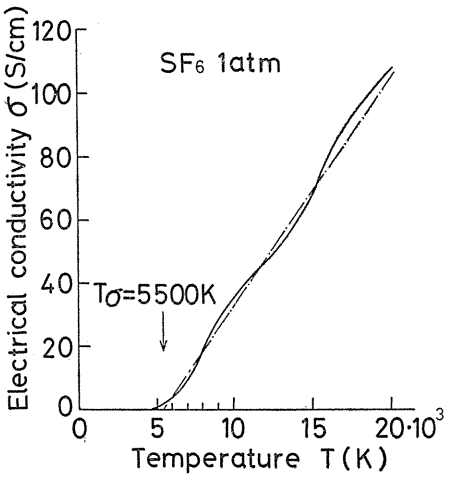

Fig. 1. Electrical conductivity of SF_6.

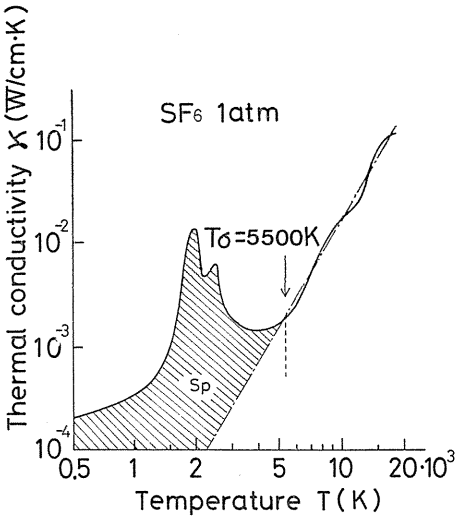

Fig. 2. Thermal conductivity of SF_6.

$$\sigma=m_\sigma(T-T_\sigma) \tag{4}$$

$$\kappa=AT^B \tag{5}$$

$$S(T)=S(T_\sigma)+\frac{A}{B+1}\left[T^{B+1}\right]_{T_\sigma}^{T}, \tag{6}$$

where m_σ, A, B and $S(T_\sigma)=\int_0^{T_\sigma}\kappa(T)dT\simeq 13.1$ W/cm are constants.

The arc current I, the integrated value of current densities all over the conducting cross-sectional area, and the thermal arc radius r_s determine the S-function distribution which finally leads to the $E-$I characteristics for different values of r_s as the special function of the column axis temperature T_0 or the corresponding conductivity σ_0 (Fig. 3). The current density $j=\sigma E$ is the unique function of σ and has its maximum value at the column axis. T_0-I characteristics are shown in Fig. 4 for several cases of different bore diameters.[16]

Recently the electronic computer enabled the numerical calculation to solve the rather complicated simultaneous differential equations. The values of σ and κ for air of 1 atm have been given by different authors independently[26] (Figs. 5 and 6). The author and his collaborators selected these values for every temperature difference of 500 K or more precisely of 100 K to obtain characteristic curves consisting of about 300 broken lines for $\sigma-T$ and $\kappa-T$ up to 30000 K. These values are put into memory for typically selected gas pressures.[22] Those examples are given in Figs. 7 and 8 for SF_6 gases of 1 and 16 atm. This technique is also

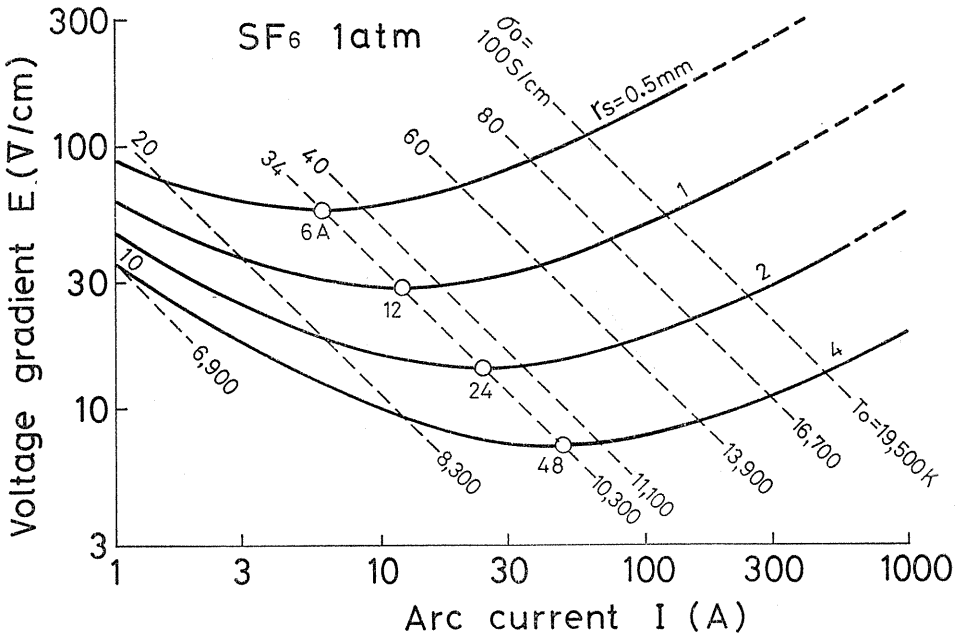

Fig. 3. Voltage gradient against arc current in SF_6 at 1 atm.

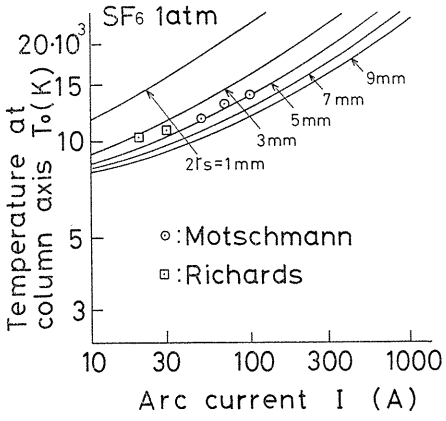

Fig. 4. Axis temperature of arc column in SF_6 at 1 atm for different bore diameters.

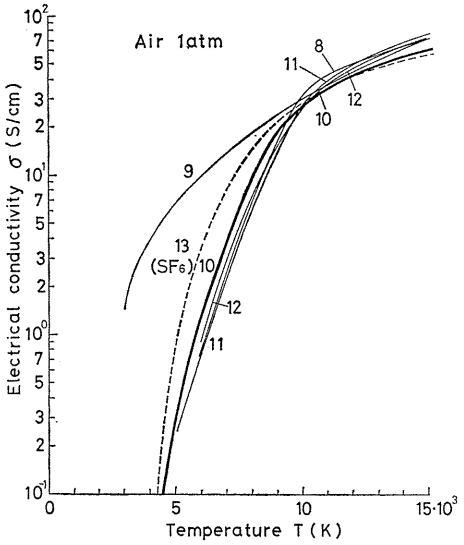

Fig. 5. Electrical conductivity of air by different authors.

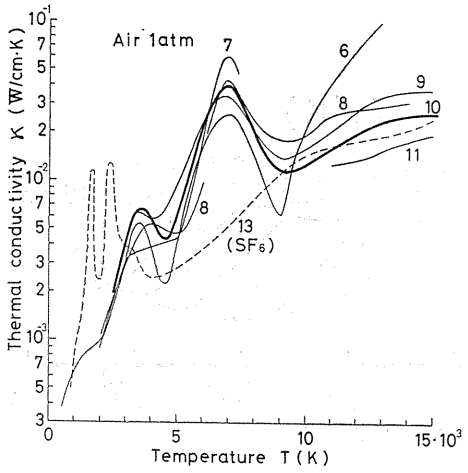

Fig. 6. Thermal conductivity of air by different authors.

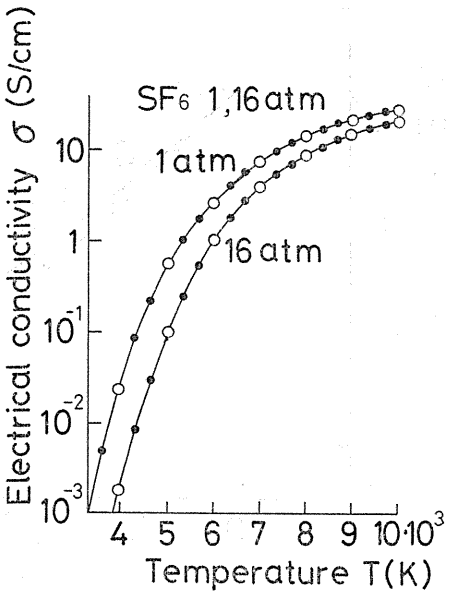

Fig. 7. Electrical conductivity of SF_6 for lower temperature regions.

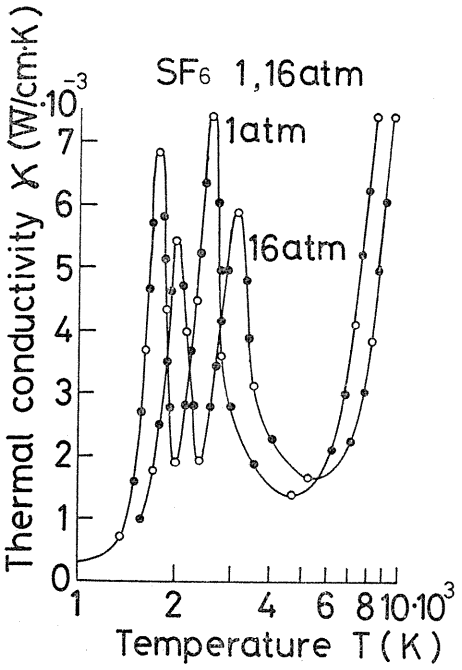

Fig. 8. Thermal conductivity of SF_6 for lower temperature regions.

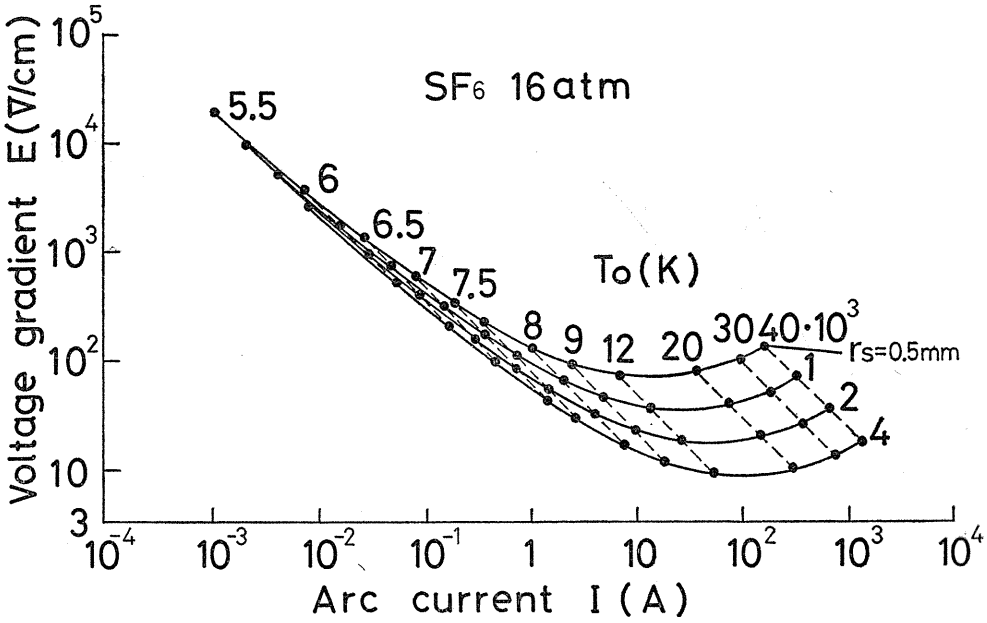

Fig. 9. Voltage gradient against wide range of arc current in SF_6 at 16 atm.

most suitable to calculate $E-I$ characteristics of relatively low temperature regions which relate to the small arc current just before the circuit interruption. Fig. 9 is an example of thus obtained $E-I$ characteristics of SF_6 at 16 atm for a wide range of arc current from 100 A to the minimm value of 1 mA, the latter case being only possible to be estimated by theoretical investigation.

4. Temperature Profile

The temperature profile may be calculated from equation (1) as the function of $\lambda=rE$ with the following boundary conditions at the column axis.

$$[dT/d\lambda]_{\lambda=0}=0, \quad [T]_{\lambda=0}=T_0 \tag{7}$$

The temperature distribution within the column is uniquely determined numerically by giving a priori the values of axis temperature T_0 and bore diameter $2r_s$.

It is reasonably assumed that, as the ordinary switching arc is burning in a gaseous atmosphere of relatively high density, the thermal energy is distributed uniformly among the elementary particles, so the arc is considered to be in thermal equilibrium. This is confirmed, when the excited copper vapour molecule is included inside the arc column, by plotting the logarithmic values of relative intensities for different wave-length of characteristic lines against excitation potentials whether the points are falling on a straight line or not. The inclination of the line is corresponding to the gas temperature of equilibrium as shown in Fig 10.[3] In this case, the temperature may be determined by a suitably selected pair of lines even if one ignores the elaborated values of partition functions concerned. Naturally the

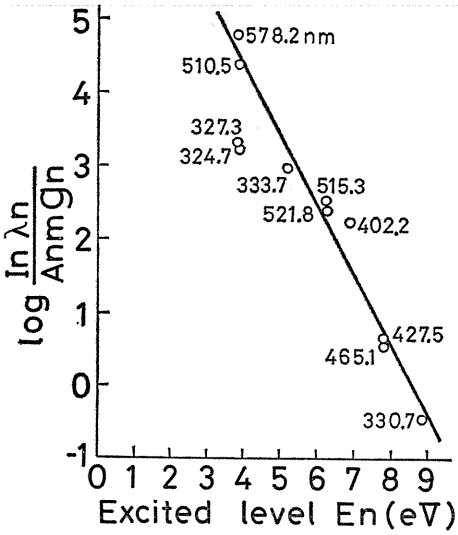

Fig. 10. Thermal equilibrium shown by line spectra of Cu(I) in air.

temperature gradient is existing in the arc column, and correspondingly the measured intensity of spectral lines must be processed by Abel transformation to obtain the real gas temperature as the function of the radius assuming the axis symmetry.

As the contents of the copper vapour are not expected to be always uniform, another method of utilizing a group of some of the rotation spectra in P-branch

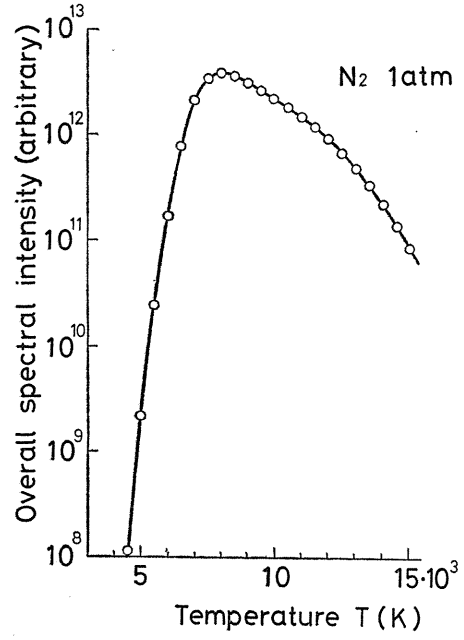

Fig. 11. Temperature dependent intensity of rotation spectra in P-branch of N_2^+ molecule.

of N_2^+ molecule is proposed by the author's group for the experimental determination of gas temperature in air containing arc. The intensity of the overall band spectra around 391.5 nm is characterized by having its maximum at the definite temperature of 8000 K, which corresponds to the point of maximum value of Abel-transformed relative intensity. By the aid of theoretically deduced result shown in Fig. 11, one can determine the temperature distribution of arc columns regardless of the uncertainty of metal vapour contents. Figs. 12 and 13 show thus obtained experimental values of temperature in relation to the theoretical distribution curves otherwise determined.

The outskirt region of the column, so called the flame, has also its own temperature gradient toward the ambient atmosphere. In this part of the arc, energy is not delivered electrically but only dissipated by radial heat transfer or eventually by forced blowout. It is rather difficult to determine the arc radius r_s theoretically, so the calculated results are preferably compared with those derived from the experiments with wall-stabilizing devices so as to give definite values of r_s.

During a period of current zero passage of AC, the time-dependent arc tem-

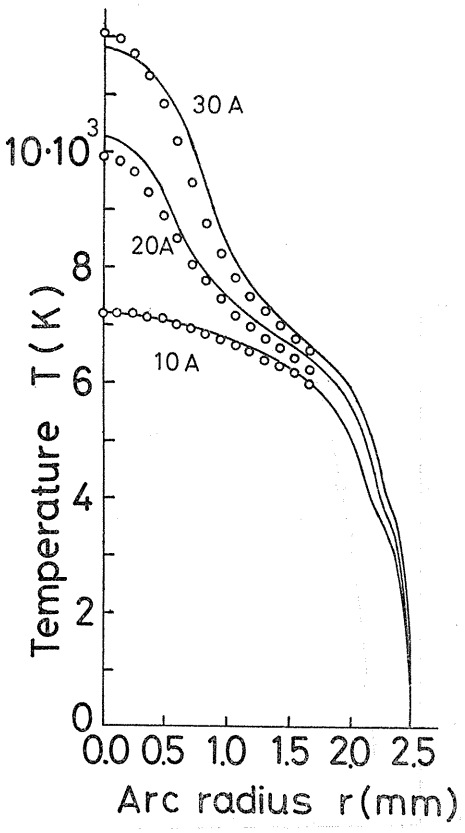

Fig. 12. Temperature distribution determined by molecular spectra with bore diameter of 5 mm.

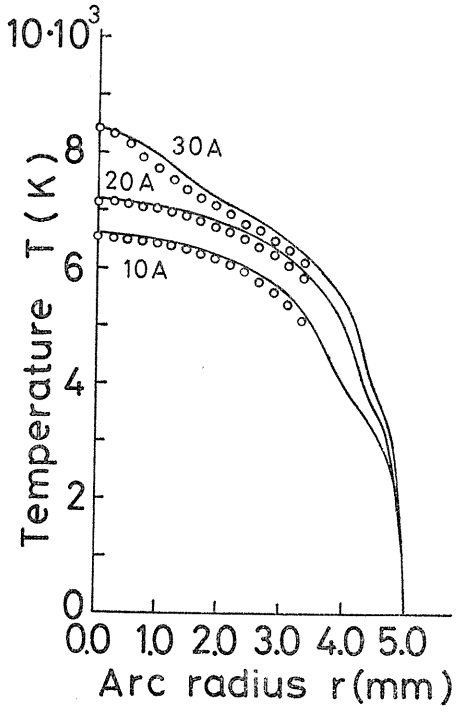

Fig. 13. Temperature distribution determined by molecular spectra with bore diameter of 10 mm.

perature will vary to some extent in lagging phase to the current intensity. The related knowledge is quite informative for the current interrpting phenomena of switching arc. These tendencies are shown in Fig. 14 as the results of preliminary experiment for arcs in SF_6 and air.

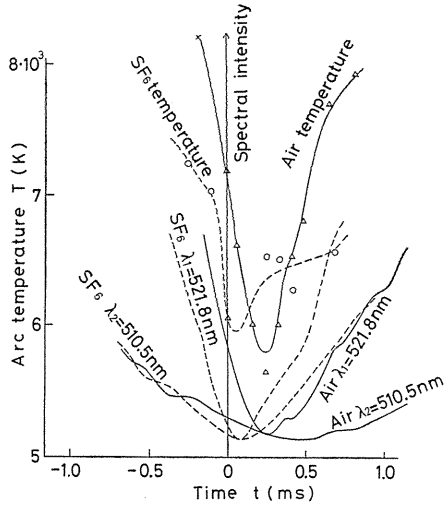

Fig. 14. Spectral intensity and arc temperature around current zero in air and SF_6.

5. Matal Vapour Contaminated Arc

The electrodes of switching elements are generally prepared by copper and its alloys. During the course of the pole opening of a switching equipment, the electrode metal may easily be evaporated into the arc column and hence the conductivity shall not be estimated from pure gas properties, but is somewhat affected by the enhanced electron density caused by relatively low ionization potential of the contaminating metal vapour.

As an example of metal vapour contaminated arc, the electron densities in high temperature air with given percentage of copper ions are calculated taking into account the thermal dissociation of oxygen and nitrogen molecules and first and second ionization of those atoms and copper.[33] The dissociation and ionization of nitrogen mono-oxide are considered at the same time. The reversible reaction equations together with their dissociation and ionization potentials and the corresponding Saha's equations are denoted by the following manner.

$$\begin{aligned} &O_2 \rightleftarrows 2O && (E_{O_2}=5.08\,eV)\\ &N_2 \rightleftarrows 2N && (E_{N_2}=9.756\,eV)\\ &NO \rightleftarrows N+O && (E_{NO}=6.48\,eV)\\ &NO \rightleftarrows NO^+ + e && (E_{NO^+}=9.5\,eV)\\ &O \rightleftarrows O^+ + e && (E_{O^+}=13.614\,eV) \end{aligned} \qquad (8)$$

$$\begin{aligned} &N \rightleftarrows N^+ + e && (E_{N^+} = 14.53\ \text{eV}) \\ &Cu \rightleftarrows Cu^+ + e && (E_{Cu^+} = 7.74\ \text{eV}) \end{aligned} \tag{9}$$

$$\begin{aligned} &O^+ \rightleftarrows O^{++} + e && (E_{O^{++}} = 35.108\ \text{eV}) \\ &N^+ \rightleftarrows N^{++} + e && (E_{N^{++}} = 29.593\ \text{eV}) \\ &Cu^+ \rightleftarrows Cu^{++} + e && (E_{Cu^{++}} = 20.29\ \text{eV}) \end{aligned} \tag{10}$$

$$\frac{n_O^2}{n_{O_2}} = \frac{(\pi m_O kT)^{3/2}}{h^3} \frac{Z_O^2}{Z_{O_2}} \exp\left(\frac{-E_{O_2}}{kT}\right)$$

$$\frac{n_N^2}{n_{N_2}} = \frac{(\pi m_N kT)^{3/2}}{h^3} \frac{Z_N^2}{Z_{N_2}} \exp\left(\frac{-E_{N_2}}{kT}\right)$$

$$\frac{n_N \cdot n_O}{n_{NO}} = \frac{(2\pi M_{NO} kT)^{3/2}}{h^3} \frac{Z_N \cdot Z_O}{Z_{NO}} \exp\left(-\frac{E_{NO}}{kT}\right) \tag{11}$$

$$\text{and} \quad M_{NO} = \frac{m_N \cdot m_O}{m_N + m_O}$$

$$\frac{n_{NO^+} \cdot n_e}{n_{NO}} = \frac{(2\pi m_e kT)^{3/2}}{h^3} \frac{2Z_{NO^+}}{Z_{NO}} \exp\left(-\frac{E_{NO^+} - \Delta E}{kT}\right)$$

$$\frac{n_{O^+} \cdot n_e}{n_O} = \frac{(2\pi m_e kT)^{3/2}}{h^3} \frac{2Z_{O^+}}{Z_O} \exp\left(-\frac{E_{O^+} - \Delta E}{kT}\right)$$

$$\frac{n_{N^+} \cdot n_e}{n_N} = \frac{(2\pi m_e kT)^{3/2}}{h^3} \frac{2Z_{N^+}}{Z_N} \exp\left(-\frac{E_{N^+} - \Delta E}{kT}\right)$$

$$\frac{n_{Cu^+} \cdot n_e}{n_{Cu}} = \frac{(2\pi m_e kT)^{3/2}}{h^3} \frac{2Z_{Cu^+}}{Z_{Cu}} \exp\left(-\frac{E_{Cu^+} - \Delta E}{kT}\right) \tag{12}$$

$$\frac{n_{O^{++}} \cdot n_e}{n_{O^+}} = \frac{(2\pi m_e kT)^{3/2}}{h^3} \frac{2Z_{O^{++}}}{Z_{O^+}} \exp\left(-\frac{E_{O^{++}} - \Delta E}{kT}\right)$$

$$\frac{n_{N^{++}} \cdot n_e}{n_{N^+}} = \frac{(2\pi m_e kT)^{3/2}}{h^3} \frac{2Z_{N^{++}}}{Z_{N^+}} \exp\left(-\frac{E_{N^{++}} - \Delta E}{kT}\right)$$

$$\frac{n_{Cu^{++}} \cdot n_e}{n_{Cu^+}} = \frac{(2\pi m_e kT)^{3/2}}{h^3} \frac{2Z_{Cu^{++}}}{Z_{Cu^+}} \exp\left(-\frac{E_{Cu^{++}} - \Delta E}{kT}\right)$$

$$\frac{2n_{N_2} + n_{NO} + n_{NO^+} + n_N + n_{N^+} + n_{N^{++}}}{2n_{O_2} + n_{NO} + n_{NO^+} + n_O + n_{O^+} + n_{O^{++}}} = \frac{78}{22} \tag{13}$$

$$n_{O_2}+n_{N_2}+n_{NO}+n_{NO^+}+n_O+n_N+n_{Cu}+n_{O^+}+n_{N^+}+$$
$$n_{Cu^+}+n_{O^{++}}+n_{N^{++}}+n_{Cu^{++}}+n_e=\frac{P}{kT} \quad (14)$$

$$n_e=2n_{O^{++}}+2n_{N^{++}}+2n_{Cu^{++}}+n_{O^+}+n_{N^+}+n_{Cu^+}+n_{NO^+}$$

$$\frac{n_{Cu}+n_{Cu^+}+n_{Cu^{++}}}{n_{O_2}+n_{N_2}+n_{NO}+n_{NO^+}+n_O+n_N+n_{O^+}+n_{N^+}+n_{O^{++}}+n_{N^{++}}+n_{Cu}+n_{Cu^+}+n_{Cu^{++}}}$$
$$=X_{Cu} \quad (15)$$

$$\Delta E=6.96\times10^{-7}\times n_e^{1/3} \quad (16)$$

where
- i : particle of ith species
- n_i : particle density (cm^{-3})
- Z_i : internal partition function
- m_i : mass
- P : total pressure
- E_i : dissociation or ionization potential
- X_{Cu} : contents of copper vapour
- T : temperature (K)
- k : Boltzmann's constant
- h : Planck's constant.

The cross-sectional areas of collision between any two of the 14 species of particles considered including electron are obtained by means of a series of elaborated calculations.

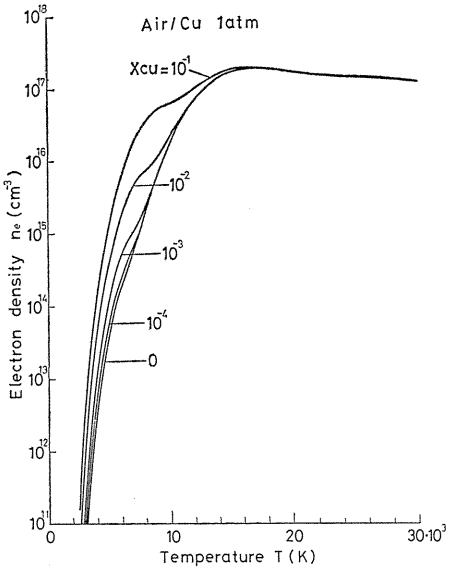

Fig. 15. Temperature dependent electron density in copper-vapour contaminated air.

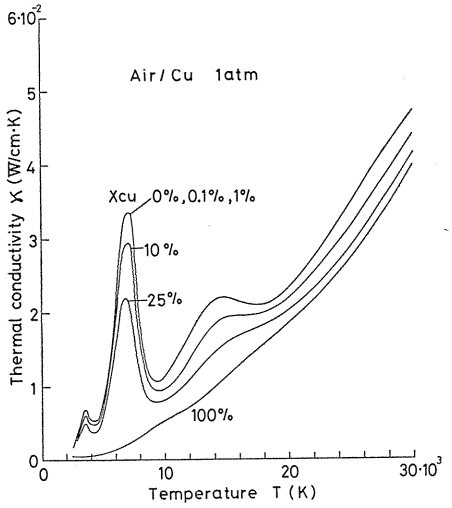

Fig. 16. Temperature dependent thermal conductivity in copper-vapour contaminated air.

The results obtained for the high temperature air of 1 atm contaminated by copper vapour of up to 10 % are shown in Fig. 15. Utilizing those values of electron densities, the electrical and thermal conductivities are deduced. The former is fairly increased by even a small quantity of contents of copper vapour especially at the temperature range below 10000 K, but, on the contrary, the latter is not distinguished by considerable reduction rate till the contents of copper is attaining some tens of percents around the dissociation temperature of nitrogen as shown in Fig. 16. The effect of the metal vapour on the $E-I$ characteristics of air arc is so represented as to reduce the generalized voltage gradient r_sE for given values of generalized current I/r_s for 100 A/cm and below. The theoretical research project on this chapter is still going on for wide range of combination of gases and parameters followed by the study of experimental confirmation.

6. Time Constant

The so-called time constant of extinguishing arc derived from the Mayr's equation or Cassie's is originary an ambiguous quantity defined as a ratio of characteristic energy to power loss considered at a given part of a dynamic arc. In spite of the fact, the Mayr's time constant is still currently available, with necessary modifications, to assess the critical characteristics of current zero phenomena of circuit-breakers. The conception of the conductance decay of an arc column during extinguishing period has been also studied from the experimental point of view.

The attemp to have a clear interpretation of the time constant of arc conductance based on the proper gas constants at high temperature is proposed by the author's group.[32] According to the study on the temperature profile, the temperature distribution inside the stabilized arc column is definitely expressed for given arc current intensity. Corresponding to the stepwise change of the current, the temperature profile will be varied from one distribution to another with necessary transient period of time. The dynamic characteristics of wall-stabilized transient arc is expressed by the following differential eqution.

$$\rho C_p\left(\frac{\partial T}{\partial t}+v_r\frac{\partial T}{\partial r}\right)=\sigma E^2+\frac{1}{r}\frac{\partial}{\partial r}\left(r\kappa\frac{\partial T}{\partial r}\right) \tag{17}$$

where
ρ : mass density
$C_p=\partial h/\partial T$: specific heat at constant pressure
h : enthalpy per unit mass
v_r : radial velocity of mass transfer
t : lapse of time.

As the parameters are solely temperature dependent quantities, the equation (17) can be numerically integrated, for convenience sake, by utilizing the values of parameters given for every temperature difference of 200K between the temperatures corresponding to the initial and the final current intensities. Examples are shown in Figs. 17 and 18 for the cases of increasing current from 19 A to 31 A and reverse direction of a stabilized air arc at 1 atm with bore diameter of 5 mm. It is observed, from these figures, that the transient time of about 100 μs is necessary to be taken into account with relatively quick response at the initial

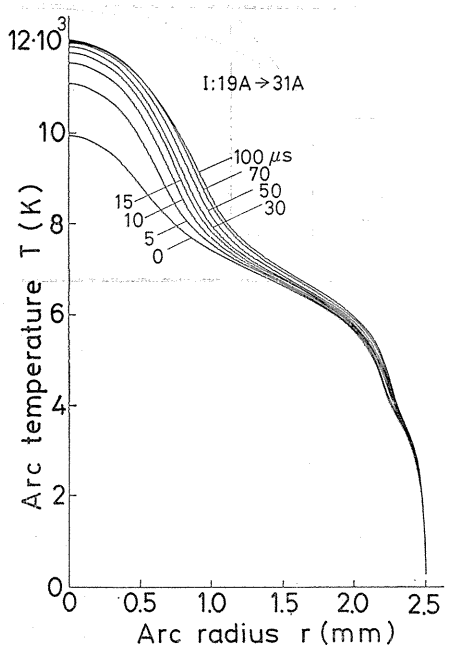

Fig. 17. Transient state temperature distribution for increasing arc current in air.

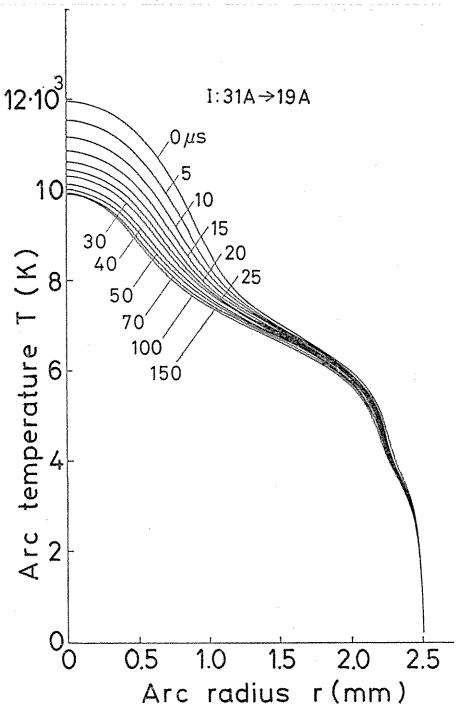

Fig. 18. Transient state temperature distribution for decreasing arc current in air.

stage of the transition. The theoretically deduced similar examples are revealed for arcs burning in air and SF_6, and the former is also compared with the experimental results with satisfactory coincidence, which means the verification of the adaptability of the theory proposed.[36]

The arc conductance $G(t)$ at the instant of time t elapsed from the moment of initial current change is expressed as follows.

$$G(t)=2\pi\int_0^{r_s} r\sigma(t,\ r)dr \tag{18}$$

This value is calculated for every instant of transient state with respect to the designated temperature distribution. The transient response of the voltage gradient $E(t)$ will be also calculated by the equation $E(t)=I/G(t)$.

As to the representation of the time constant $\theta(t)$ of the transient arc conductance thus obtained, the instantaneous value is defined by the following equation relating to Fig. 19.

$$\theta(t)=\{G_s-G(t)\}/(dG/dt) \tag{19}$$

where G_s : conductance value of the final state.

The defined time constant $\theta(t)$ at any moment means the time to be required to attain the final conductance value from the moment considered provided that the

instantaneous value of the time derivative of the conductance is kept constant. $\theta(t)$ might be constant if the exponential change of conductance value is expected. Unfortunately, this is not a constant in the true sense of the word for the ordinary transient arcs investigated. Nevertheless, those values of $\theta(t)$ observed in the above mentioned examples are scattering around the average value of 20 μs. The correlation between $\theta(t)$ and the instantaneous axis temperature T_0 is suggested to hold good in these cases.

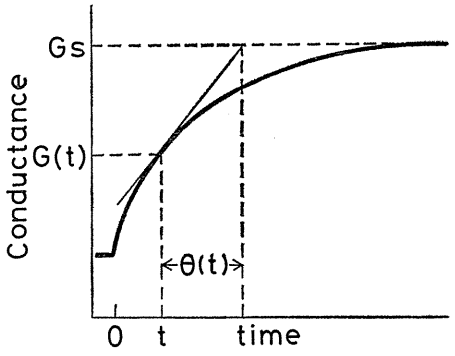

Fig. 19. Definition of time constant of arc conductance.

7. High Temperature Breakdown

In most of the cases of switching arc phenomena the successful current interruption is aimed in an atmospheric condition of high temperature just after the recognizable current flow ceases to exist. Under these conditions, the breakdown characteristics must be studied from the viewpoint of the restoration of the insulation strength of the conducting media instead of the initiation of the conduction phenomena inside the gases of ambient temperature as is commonly interested in.

The electric breakdown in high temperature gases has been analysed in a space of uniform field intensity E_0 where the existing initial current density J_0 may be increased into the balanced value of current density J by the externally applied voltage.[30) 37)] The critical breakdown voltage V_B of those gases is calculated by the runaway condition of the current density: $J_0/J=0$.

$$E_0=\frac{DP}{\ln CPd-\ln\ln\left(\frac{1+\gamma}{J_0/J+\gamma}\right)} \tag{20}$$

$$V_B=\frac{DPd}{\ln CPd-\ln\ln(1+\gamma^{-1})} \tag{21}$$

where
P : total gas pressure (mmHg)
d : gap length between electrodes (cm)
γ : ionization rate of secondary emission
C, D : constants.

The current density produced by thermionic emission from high temperature electrode is much more predominant than that derived from thermal ionization of gases for the temperature range under consideration, so J_0 is understood to be supplied uniquely from the electrode surface corresponding to the temperature thereof. After having been examined the values of steady state current density as the function of J_0 and applied voltage, the equation (21) is solved by introducing the

properly selectdd values of constants and parameters as indicated below for nitrogen where the mobility of positive ion μ_+ and that of electron μ_- are considered.

$$D=270.0\ (cm^{-1}\cdot V\cdot mmHg^{-1})$$

$$C=10.0\ (cm^{-1}\cdot mmHg^{-1})$$

$$\gamma=1.0\cdot10^{-4}$$

$$\mu_+=2.17\cdot760/P\ (cm\cdot V^{-1}\cdot s^{-1})$$

$$\mu_-=\mu_+\cdot10^3\ (cm^2\cdot V^{-1}\cdot s^{-1}) \tag{22}$$

Fig. 20 shows the calculated results of breakdown voltage together with the experimental ones for nitrogen gas up to 1500℃ for some different combinations of constant pressure and gap lengths. In some of the cases, the remarkable lowering

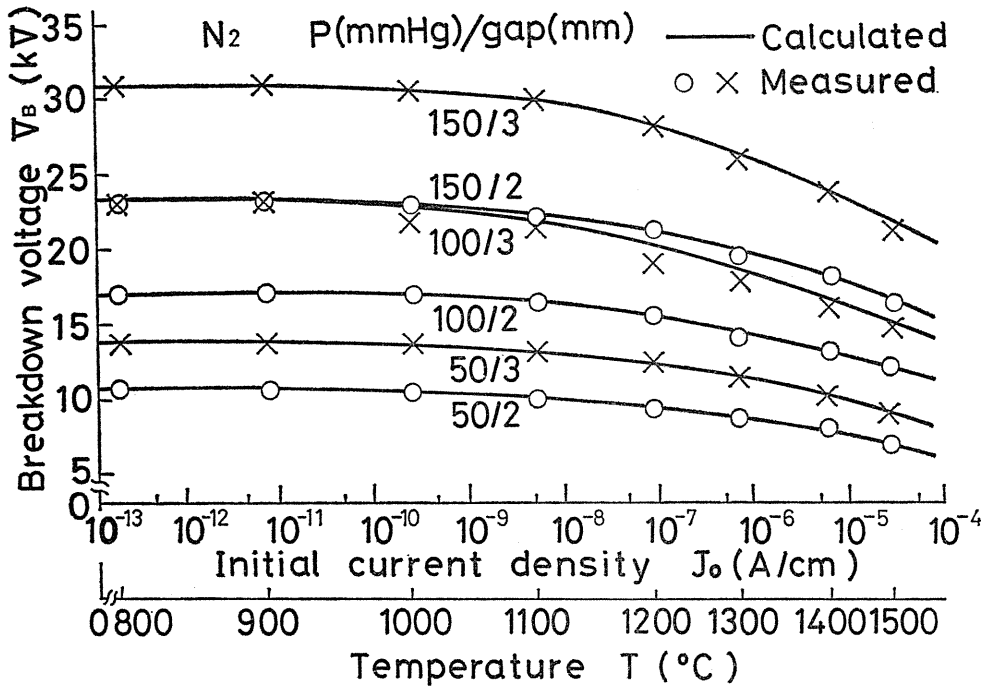

Fig. 20. High temperature breakdown voltage in nitrogen.

of the breakdown voltage is observed in the temperature range above 1100℃. The experiment is carefully carried out inside the pressure-controlled chamber with an external heating device to maintain the electrodes and the intervening gap space at an uniform temperature.

The similar calculation and experiment are extended to the common gases such as argon etc. The idealized experimental arrangement is quite effective to support

the theoretical deduction of the problem but is not sufficient to explain the recovery rate of the insulation strength from the switching arc conditions with unequal temperature distribution between gases and electrode surfaces.

8. Spiral Arc

The current conducting arc path is easily driven dynamically as the result of electromagnetic forces imposed upon every part of the conducting element. There have been so many devices to prevent the arc path from coming into contact with the undesirable parts of the materials used in power systems so as to avoid their deterioration caused by high temperature of the arc. Other devices are realized to elongate the arc path ingeniously to manage the cooling effect may be accelerated as quickly as possible for the purpose of current interruption. In AC circuit-breakers, the so-called rotary arc device is introduced utilizing the effect of the dynamic forces of the longitudinal magnetic field on the arc path burning between the two coaxial cylindrical electrodes.

The concrete idea of the "spiral arc" is first proposed by the author several years ago to interrupt the direct current successfully without utilizing any special devices such as high-speed blowout systems etc.[23] Of vital importance is to push away the arc path between the electrodes outward as soon as possible at the initial stage of the pole separation. Once a small looping path is there happened to occur, the externally applied electromagnetic forces parallel to the electrode axis will affect to enlarge the loop radius of the arc path continuously. At the same time, the foots of the conducting arc on both surfaces of the electrodes of different polarities would be forced to move away oppositely. The specially designed electrode configuration for this purpose is shown in Fig. 21.[34] Compared with the electrodes of cylindrical type (a), the repulsion type (b) is more effective and confident as the initial arc path is easily pushed away by the effect of the opposite-direction current flow on each top of the separating electrodes. As the sectional projections of the extremities of both electrodes are cylindrical, the foots, more precisely the electrode-column junctions, of the arc path will rotate in the reverse direction during the course of gap separation, which, at last, leads to the several turns of spiral arc between the electrodes accompanied by everlasting expansion of the loop radius. The elongated arc path thus obtained and the cooling effect of the moving arc result in a considerable rise of voltage drop so as to limit the intensity of the direct current until successful interruption. To determine the instantaneous spatial length of the arc path, it is necessary to observe

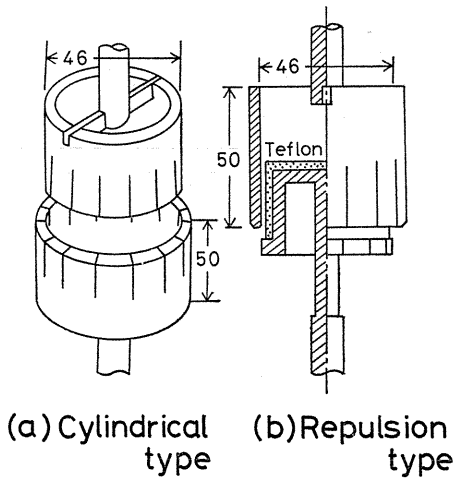

Fig. 21. Specially designed electrode configuration.

experimentally the expanding profiles of spiral arc from end-on and side-on directions at the same time. A two-dimensional photographic device is utilized, for this purpose, the schematic representation of which is shown in Fig. 22 with special

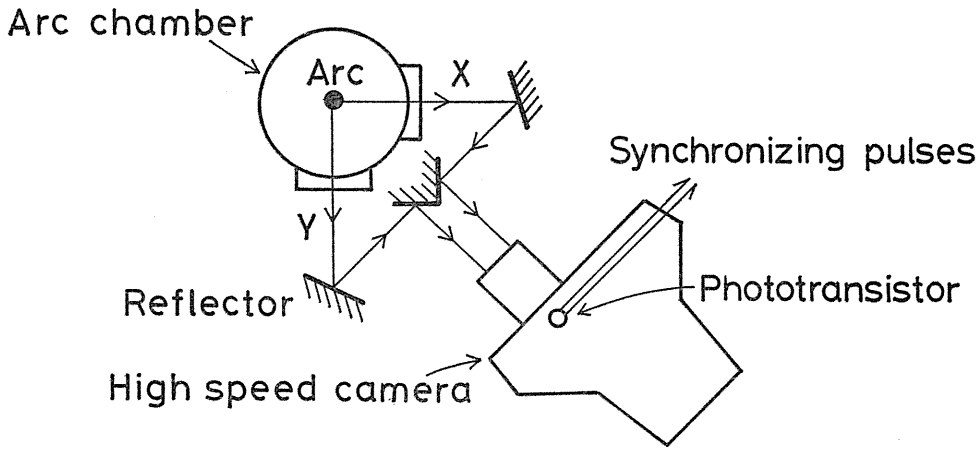

Fig. 22. Schematic representation of two-dimensional photographic device.

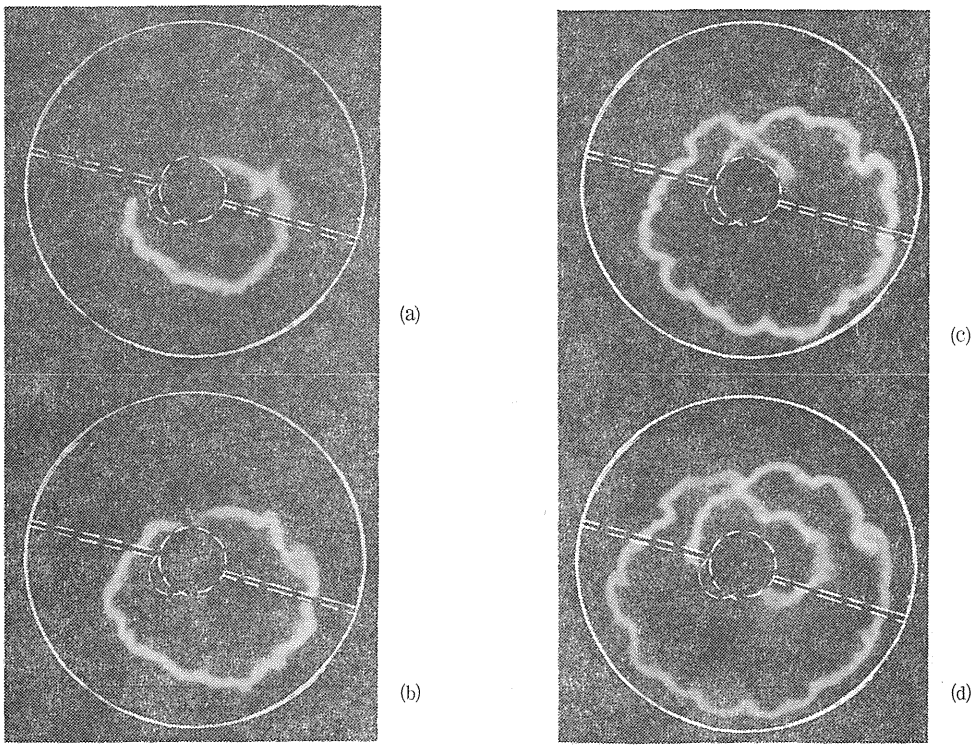

Fig. 23. Evolution of spiral arc of DC 2.8 kV-926 A in SF_6 at 6 atm after pole separation. (a) 12.7 ms, (b) 13.1 ms, (c) 13.5 ms, (d) 13.8 ms.

consideration of synchronized recordings of a cathode-ray oscilloscope and an ultra-high speed framing camera.

An example of the direct current interruption by means of the spiral arc device is shown in Fig. 23. A direct current of 2.8 kV -926 A is successfully interrupted inside the arc chamber containing SF_6 gas of 6 atm within a short period of less than 15 ms as shown in the figure, where the growth of the spiral arc path and the rotating spots in opposite directions on both electrode surfaces are clearly observed.[31] Naturally, the voltage gradient of the spiral arc against the current intensity is much higher than that of the free-burning one, the conditions otherwise being unchanged.[35]

9. Emission of Radiation and Optical Diagnostics

The radiated energy from the arc column may not be neglected especially when the heavy current arc is burning in relatively high pressure gaseous atmosphere as is offen the case with the arc in the actual switching equipment. The energy balance equation (1) is rewritten as follows for the steady state conditions where the emitted intensity of radiation per unit volume is denoted by U.

$$\sigma E^2 = U - \frac{1}{r}\frac{d}{dr}\left(r\kappa\frac{dT}{dr}\right) \tag{23}$$

Inside the high temperature air of 1 atm, the distinguished value of $U(T)$ is recognized at the temperature higher than 15000 K as shown in Fig. 24. In case of the high pressure air of e.g. 10 atm, $U(T)$ will be somewhat 100 times greater than that of 1 atm with the transport properties such as electrical and thermal con-

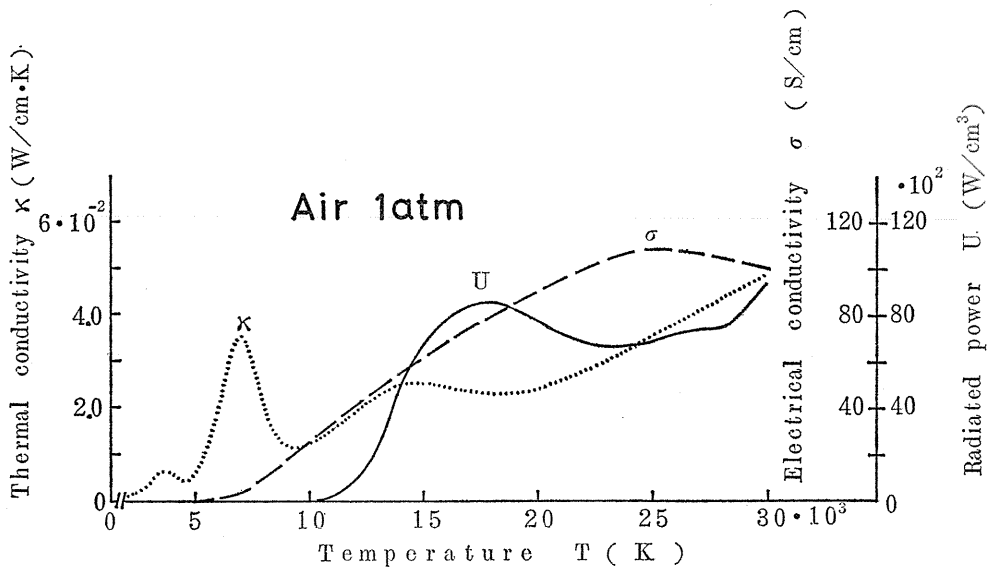

Fig. 24. Radiated power compared with other transport constants of air.

ductivities $\sigma(T)$ and $\kappa(T)$ being scarcely changed.

The voltage grandient against current characteristics with radiation considered are obtained from equation (23) through the numerical calculation by the similar manner as explained hitherto. In these cases, the hypotheses are so taken into account that (a) the arc core and the flame are considered to be optically thin such that the self-absorption of radiation is neglected there, and (b) the continuum radiation source strength is sufficiently predominant to the line radiation one to the extent that the latter may be neglected for the high temperature range considered. Preliminary results thus obtained theoretically for 1 atm air arc are shown in Fig. 25. All the characteristic curves for different bore diameters are equally

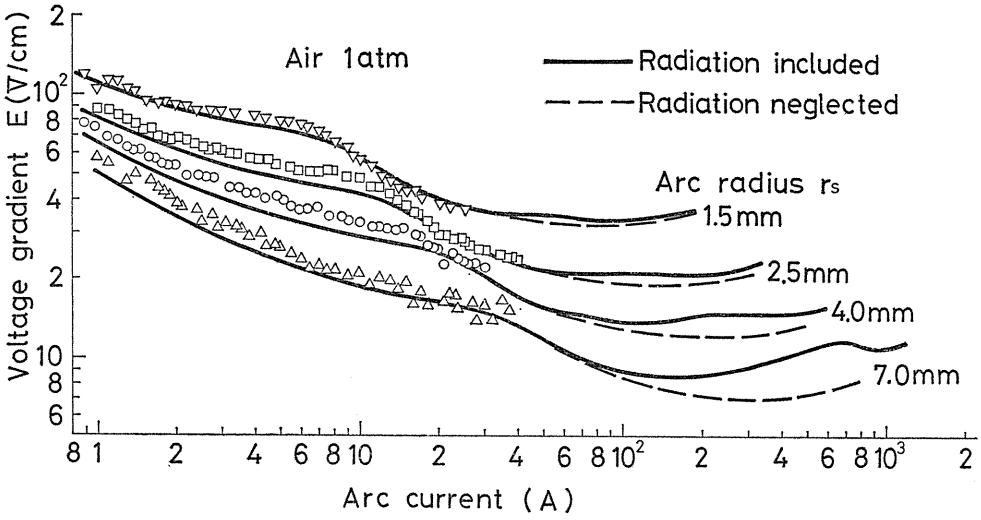

Fig. 25. Comparison of calculated (lines) and measured (spots) E-I characteristics in air at 1 atm.

affected by the dissociation of nitrogen molecule to give rise to an enhancement of the voltage gradient for the current range below 50 A, and this tendency is also the true above 100 A as the result of radiated energy from the arc column especially for relatively larger bore diameters. The dominant effect of the radiation power is observed for the high pressure air arc of 10 atm as shown in Fig. 26, where the dissociation peaks are almost disappearing and the axis temperatures are surprisingly falling down to establish a balanced condition of equilibrium between input power and dissipation. Thus the high power electric arcs commonly found inside the quenching chamber of circuit-breakers are theoretically investigated. Again, some examples of the temperature profiles affected by the radiation power are shown in Fig. 27. Not only the axis temperatures but also the temperature distributions are seriously disturbed by the radiated energy from the central parts of the arc column. The similar analysis on the radiation power is also extended to the cases of the arcs burning in high pressure SF_6 gas.

Optical diagnostics are quite effective measures to reveal the properties of the arcing phenomena because the emitted radiation of lines and continua from the

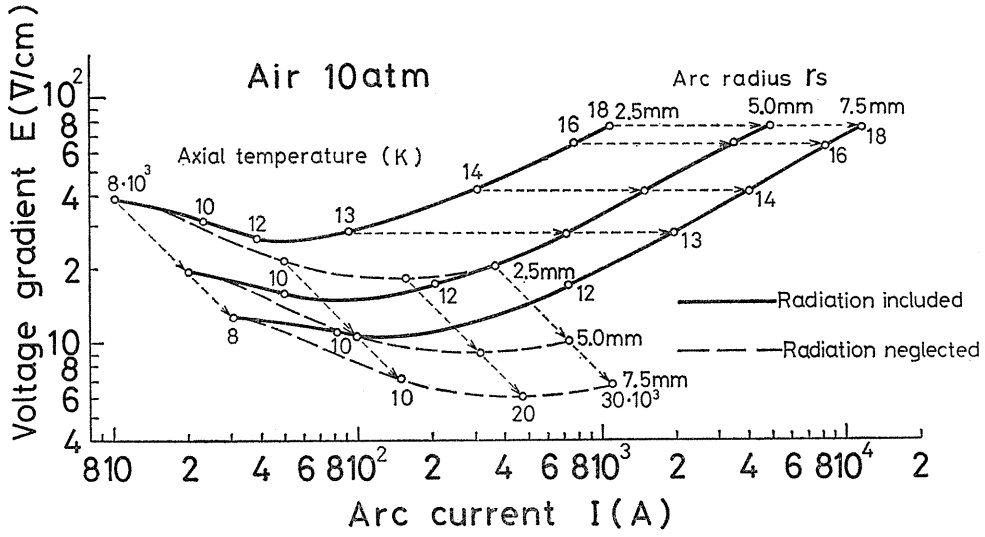

Fig. 26. Calculated E-I characteristics in air at 10 atm.

column is faithfully corresponding to the characteristic behaviour which is taking place inside the domain of arc discharge. To analyse the temperature distribution of the outskirt part of the arc, where the charateristic emission of light is not expected, Schlieren method is commonly used to grasp an overall picture of the

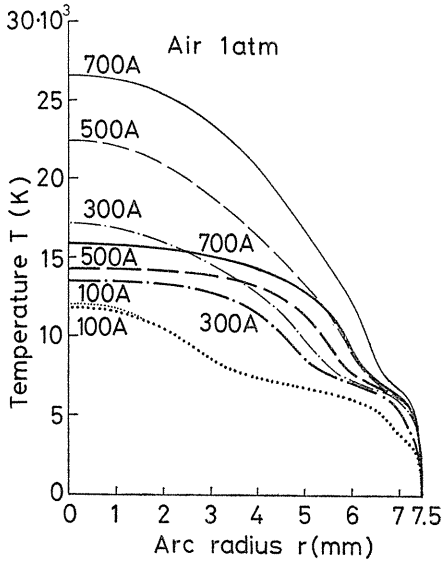

Fig. 27. Calculated temperature profiles inside arc column in air at 1 atm: thick line-radiation included and thin line-radiation neglected.

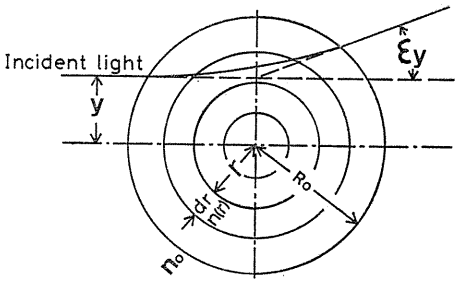

Fig. 28. Deflection angle of a light beam through distributed temperature field.

arc space. This arrangement is preferable to observe the boundary layer of the high temperature range around the arc column qualitatively, but is not convenient to deduce from the results obtained the actual temperature distribution quantitatively by processing the measured data.

A proposal called "light beams deflection method" utilizing a bundle of parallel beams of projected light through the arc space is realized to determine the instantaneous temperature distribution experimentally with sufficient precision.[19] An incident light beam of small diameter introduced perpendicularly to the column axis with a distance of y apart shall be deflected toward the outside after passing through the distributed temperature field around the column as shown in Fig. 28. The resultant deflection angle ε_y observed from the opposite side of the light source is expressed by equation (24).

$$\varepsilon_y = \frac{2}{n_0}\int_y^{R_0} \frac{dn}{dr}\frac{y}{(r^2-y^2)^{1/2}}dr \tag{24}$$

where n : refractivity of gas at temperature $T(K)$ and pressure P(mmHg)
n_0 : refractivity at ambient temperature $T=300$ (K)
R_0 : utmost radius of the thermal territory.

For relatively low temperature range of the atmospheric air where the dissociation of the constituent molecules can be neglected, the relation between the temperatures T_k and T_{k+1} of two adjacent parts of the flame at the k-th layer of the equally divided annular section by small element of radius Δr is shown as follows.

$$\frac{1}{T_k} = \frac{1}{T_{k+1}} - \frac{1}{0\cdot 08}\left(\frac{dn}{dr}\right)_{k+1}\Delta r \tag{25}$$

The combination of the equations (24) and (25) will determine the temperature gradient of the non-luminous part of the column by substituting the measured values of the ε_k of the k-th layer of properly divided radius and R_0. Examples of photographs indicating the deflected images of light beams compared with those

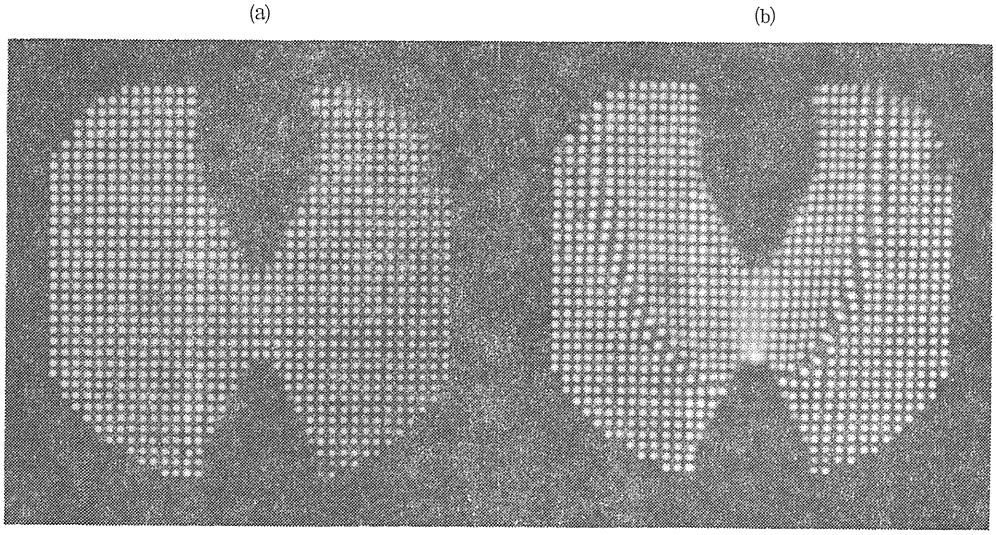

Fig. 29. Images obtained by light beams deflection method.
(a) without arc, (b) with arc.

through the uniform temperature field are shown in Fig. 29.

Another example of the photographic diagnostics is referred to for the case of an arc discharge of extremely-long gap. The natural lightning might be triggered to discharge by rockets and wires for the purpose of protecting the exposed electrical installations such as transmission towers and cables. Of course, the lightning strokes against conducting lines and elevated ground wires of the transmission route frequently provoke the serious faults and damages of the electric power systems, and the detailed researches on the inversed flashover from the tower to the lines and the similar arcing phenomena produced relating to the lightning discharge are quite necessary to protect the whole systems safely and to maintain the stable power supply of highest quality. The research project team has been organized and presided by the author to develop the triggering technique of the natural lightning discharge and to prevent the accidents from happening to occur through its application.[28] Fig. 30 shows the lower part of the triggered lightning discharge of 1800 A with negative polarity extending up to a height of more than 800 m above ground. The experiment is effected by the author's group in December, 1977 at the Kahokugata reclaimed land situated in the northen district of Central Japan near Kanazawa.

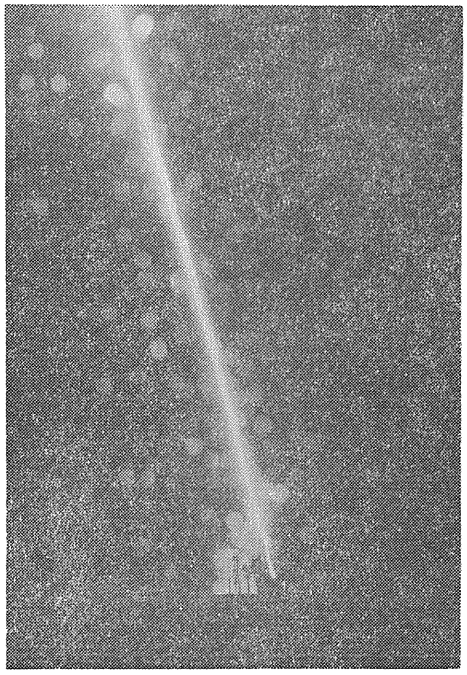

Fig. 30. Luminous conducting path of triggered lightning discharge of 1800 A with negative polarity.

10. Engineering Requirements

10. 1. Restriking Voltage

Just after the complete current interruption, the restriking voltage or, the more generally speaking, the transient recovery voltage (TRV) will break out

between the poles of the separated electrodes with relatively servere rate of rise. The waveforms may be sinusoidal for breaker teminal fault (BTF) or linearly uprising for short-line fault (SLF) according to the conditions. The former corresponds to the resonance frequency of a set of capacitances and inductances of the local and lumped circuit elements on both sides of the circuit-breaker. The latter is mainly resulting from the reflection of the travelling waves on the line side of the breaker. In case of the small-current interruption of inductive and capacitive circuits, the restriking voltages are also significant for the sake of the inherent phase difference of commercial frequency between the recovery voltage and the interrupting current.

The rated maximum rate of rise of restriking voltage is 3 kV/μs with frequencies covering from 1.4 to 20 kHz but the much more severe cases may be encountered as in the case of unexpected abnormal fault conditions not yet covered by standards. At the moment of current interruption, the residual current of the order of one thousandth of the intensity of interrupted current will sometimes follow to pass through the high temperature gap spacing. This phenomenon is desirable for the completion of the switching-off operation if the existing ions and electrons are swept away onto the electrodes, but is not acceptable when the ionization by collision will successively increase the conducting current between the poles. This is why the phenomena concerning the high temperature breakdown are necessary to be made clear relating to the thermal reignition of the switchgear. The so-called voltage breakdown is also a troublesome thing possibly comes to exist at the build-up stage of the transient recovery voltage after some intervening period of tentative interruption.

Initial transient recovery voltage (ITRV) observed within a time lapse of less than several micro-seconds after interruption is so affecting to delay the occurrence of normal TRV by the existence of small amount of stray capacitance or to accelerate by lumped inductance. Whether the opening gap is withstanding against the restriking voltage or not must be discussed from the standpoints of the interaction between the arc properties and the circuit configurations. The switching overvoltages thus produced after the current interruption is decisively important for determining the insulation coordination levels in the EHV systems exceeding the nominal voltage of 275 kV.

10. 2. Fault Current Interruption

The actual current intensity to be interrupted at present in case of the grounded fault in highest voltage transmission systems is an order of 50-80 kArms. As the alternating current is always managed to be interrupted around the current zero period, its crossing speed through zero point is likely to have an important significance to find out the chance of current interruption. The current ramp corresponding to 50 kA at 50 Hz is equal to 22.2 A/μs which is also corresponding to 5 kA at 500 Hz. Even if the ramp speed is the same, the heavy current loop of 50 Hz will probably impose the more severe problems of thermal inertia upon the interrupting ability of the arc space at the moment of zero passage just coming along 5 ms later on. The effect is of vital importance for the case of the modern extinguishing chamber of puffer-type nozzle arrangment where the expected pressure rise and the undesirable nozzle clogging are critically bordered with each other. The theory studied on the time constant of the arc in chapter 6 of this article shall be applied at first to clarify the transient property of the arc conduc-

tance between the electrodes for steady state current zero passage of commercial frequency fully taking into account the thermal inertia of heavy current loop. Next, the analysis will be extended to the interrupting conditions of the current for different types of circuit-breakers with necessary modification of consideration.

The arc discharges in the vacuum-type circuit interrupters show the wide-range positive characteristics of voltage against current relations, that is to say the arc voltage is falling down in accordance with the current ramp toward zero. The characteristics will be utilized successfully to interrupt the fault current by parallel connection of circuit-breakers of this type so as to divide the total current practically equally to each of the apparatus. At last, the full fault current will be interrupted by n-groups of breakers in parallel with individual interrupting capability of one n-th of total power. The possibility of parallel interruption by conventional circuit-breakers of high quality such as gas-blast and air-blast types must be analysed theoretically as well as experimentally hereafter referring to the E-I characteristics of the arc concerned. Thus the most difficult problems to adapt the limited maximum capability of circuit-breakers to the ever increasing values of fault current in electric power systems will be solved appropriately.

The metal vapour included in an air arc has been analysed in the preceding chapter as to have a significant effect on the decrease of the thermal conductivity of the gas mixture resulting from the fact that the reaction energy transport caused by the dissociation of nitrogen molecules is strongly hindered. The voltage gradient of the copper-vapour contaminated air arc may be lower than that of the intrinsic air for a range of small values of current intensity corresponding to those just before interruption. The suppression of the temperature rise inside the arc column due to radiated power ought to have significant effects on the process of current interruption. These problems are left to be carefully analysed to draw out the individual solutions or the combined consequences for finding the feasibility of the fault current interruption.

10. 3. Direct Current Interruption

The direct current power systems are becoming more and more practical in every corner of the world to transport a great deal of electric energy over a long distance of 1000 km for example or to connect the two separate gigantic power networks by under-sea cable routes. The major technical advantage of these systems is found in the fact to be able to avoid the effect of line capacitances which is fatal to the alternating current transmission. Unfortunately, the DC transmission networks are normally realized only by the combination of a simple two-terminal system owing to the lack of the applicable DC circuit-breakers of practical scale at present.

Of course, there have been many attempts to interrupt the direct current of several thousands of amperes by the application of the conventional type AC breakers. For this purpose, complicated devices must be introduced to commutate the main current into the auxiliary circuit so as to obtain the instantaneous chance of current zero in principal circuit finding the opportunity of current interruption by AC breakers. As the auxiliary circuit is generally consisting of the resistors and capacitors equipped with additional auxiliary breakers, it might be able to absorb the energy dissipated by the transmission line and to limit the magnitude of the current so as to be easily interrupted. The electromagnetic energy to be disposed of at the moment of direct current interruption is an order of some mega-joules

which is more than ten times greater than the corresponding electrostatic one.

Vacuum switches and air-blast circuit-breakers have been studied to construct DC interrupters and the test results on the practical transmission lines were published. Liquified SF_6 gas was also utilized for one of the prototype of the quenching chambers proposed.

The author's proposal as shown in this article to interrupt the direct current by spiral arc is another system of controlling the current to be switched off. Nevertheless, the economically acceptable DC circuit-breakers with the object of working on daily services are not yet brought into existence. Only the DC breakers called metallic return transfer breakers (MRTB) are now under the consideration of practical utilization. When the converters of one of the poles of symmetrical transmission system to ground is out of service, the faulty pole is, at first, deenergized and disconnected from the circuit and finally the intermediate ground return current shall be diverted into the conductor of faulty pole by the aid of MRTB. The breaker is requested to commutate the nominal current safely under a relatively low terminal voltage corresponding to the resistance drop of the circuit.

10. 4. Reliability of Circuit-Breakers

According to the world-wide statistics on the major and minor defects of the circuit-breakers in service, the failure rate is continuously on the decrease year by year from several percents of about ten years ago to less than one percent at present. About 85% of the failures and defects are said to be coming from the mechanical origin derived not from the design mistake but from the misconduct during the course of manufacture. The well-arranged quality control system is most effective to produce a series of circuit-breakers of good performance. As a circuit-breaker is generally constructed by the combination of so many kinds of elementary parts of different reliability, it is necessary to minimize the number of the constituents so as to maintain a high-grade reliability of the completed apparatus.

The experiences accumulated in the engineering techniques such as designing, manufacturing and testing on manufacturers' side and installation and maintenance on utilities' side might be reflected in the construction of new types of circuit-breakers rated for the unexperienced highest current and voltage levels. One of the solutions for this aim is to apply the same sorts of constituent parts both in the present and future requirements of EHV and UHV systems.

Any sorts of the faults and damages brought about inside the power systems must be eliminated by the protecting mechanisms of suitably installed circuit-creakers of the network. One of the most important problems to be solved about the current interrupting phenomena concerning the reliability is the effect of the multi-strokes of lighthing discharge superimposed on the opening course of a circuit-breaker. This is a period of most vulnerable condition for the arc space, and the interrupting mechanism may be once more theoretically analysed from the viewpoint of high temperature withstand characteristics of extinguishing media disturbed by the simultaneous application of impulse voltages. Another attempt to realize the types of circuit-breakers totally exempt from maintenance and supervision is also directed to the improvement of reliability.

10. 5. Testing by Synthetic Method

The nominal interrupting capacity of a circuit-breaker must be verified by an appropriate procedure at the testing station with sufficient background of power supply. The actual high power circuit-breaker of 500 kV for example consists of two or three unit breaking points in series per phase to interrupt the probable maximum fault current. The only one unit test or the test for the combination of some of the units in series of one phase of a circuit-breaker are now commonly performed because the full power interrupting test of three-phase or even one complete phase arrangement is practically impossible from the economical point of view as to supply the short-circuit current and the full recovery voltage at the same time. The maximum rating of the breaking unit is now corresponding to a set of 63 kA-220 kV or so which may be, at least, tested by synthetic method.

Among the proposed schemes, the current injection method is an efficient test procedure utilized in most of the testing stations in the world. This is composed of two energy sources: the current source and the voltage source. The former supplies the test current of full intensity under the voltage level sufficient to maintain the arc voltage during the short-circuit period and may be the short-circuit generators or the actual operating power systems. The latter is an artificial power source with charged capacitor banks to supply generally one tenth of the full load current for a short period of time at a frequency of ten times greater than that of current source with the ability of producing necessary transient recovery voltage after interruption. The two sources are so combined as to be superimposed at the end of the interrupting current loop with an overlap period of 90 degrees of the phase angle of the current supplied by voltage source. The examples of the maximum power of those test equipments are shown as follows: 20 kV - 100 kA or 15 kV - 200 kA continuous supply at 50 or 60 Hz for current source and 400 kV - 7 kA or 800 kV - 20 kA during a short period of time of about 20 ms at 500 Hz for voltage source. If a high-speed reclosing test of circuit-breaker is requested, the voltage source of this kind may be multiplied corresponding to each additional current zero passage.

Now the condition of the successful interruption of a breaker is certified by the test results obtained from the probability distribution of multiple times interrupting tests, and it takes so much time and expenses even for the test of a part of the circuit-breaker. Recently an idea is raised to test the circuit-breakers more efficiently by introducing appropriate arc models for different types of interrupting devices currently used in relation to the external circuit conditions. The theoretical treatments of arc characteristics studied in this article are all supposed to be quite useful to give a definite conception of the necessary arc model. On the other hand, a trend is coming about that all the operating capabilities such as closing, reclosing and fault clearing of any kind, relating to the fully equipped circuit-breakers, are considered to be the objectives of the testing by synthetic method.

11. Summary

How to unite the technical fundamentals and the engineering requirements most effectively is an important subject to arrive at a modern technical achievement.

By a series of results obtained from the research items studied in this article, a great deal of contributions are expected in the domain of fundamental interpretation of switching arc phenomena, which, in turn, plays the valuable role of developing the new types of switching devices based on theoretical background and of establishing reasonable testing method of circuit-breakers. Many problems are still left to be solved for the detailed application of the theory. Analyses concerning the time constant just before the current interruption assisted by a violent stream of gas flow and the following residual current phenomena are some of the examples. There is also a quite naive question: is the externally driven arc column considered as a sort of high temperature moving stick of solid state or something like the travalling wave of high temperature energy?

Acknowledgement

The author is greatly indebted to Professor Y. Kito of Nagoya University for his everlasting collaboration and friendship on the realization of present scheme extending over a period of more than 20 years. The author is also grateful to Miss K. Kato and Mr. K. Oshima who have kindly prepared the typescript and the figures in this article.

Literature

1) I. Miyachi: Arc Characteristics in SF_6 Gas, Hoden Kenkyu **23** (1965), 7-19.
2) I. Miyachi: Arc Discharge Characteristics in Electronegative Gases, Hoden Kenkyu **29** (1967), 65-84.
3) I. Miyachi, Y. Kito and K. Okada: Distribution of Gas Temperature and Electrode-Metal Vapour Density in an Electric Power Arc Determined by the Rediated Spectral-Line Intensity, JIEE Japan **87-945** (1967), 1227-1234.
4) I. Miyachi and K. JayaRam: Estimation of the Quadratic Stark Shifts in Cu I, J. Phys. B. **2-2** (1969), 425-427.
5) I. Miyachi and K. JayaRam: Laser Field Stark Effect in Potassium and Caesium, Acta Physica Polonica **A37** (1970), 151-154.
6) I. Miyachi, Y. Kito and R. Miyata: Dependence of Maximum Arc-Energy on the Testing Voltage Observed in a Current Limiting Fuse, JIEE Japan **90-4** (1970), 631-639.
7) Y. Kito, T. Inaba and I. Miyachi: Voltage Gradient along SF_6 Arc Column Making Use of its Looping Tendency, Int. Conf. on Gas Discharges (London), IEE Pub. **70** (1970), 324-327.
8) I. Miyachi and K. JayaRam: A Stabilized Metal Vapor Arc Device, Rev. Sci. Inst. **42-7** (1971), 1002-1004.
9) I. Miyachi, T. Inaba and Y. Kito: Voltage Gradient of Wall Stabilized High Pressure SF_6 Arcs, 10th Int. Conf. on Phen. in Ionized Gases (Oxford), **324·13** (1971), 210.
10) I. Miyachi and K. JayaRam: Kinetic Temperature, Distribution Temperature and Electron Density in a Stabilized Copper Vapour Arc in Air, 10th Int. Conf. on Phen. in Ionized Gases (Oxford), **323·5** (1971), 180.
11) T. Inaba, Y. Kito and I. Miyachi: Thermal and Electrical Properties of Heavy Current Arc Column in SF_6 Gas, Z. Physik **247** (1971), 227-237.
12) I. Miyachi and K. JayaRam: Theoretical Estimation of the Spectral Line Broadening Constants of Copper I, Acta Physica Polonica **A40** (1971).

13) T. Inaba, Y. Kito and I. Miyachi: Voltage Gradient along an Arc Column in SF_6 Carrying Heavy Currents, Trans. IEE Japan **92-4** (1972), 47-A21, 179-188.
14) T. Sakakibara, Y. Kito and I. Miyachi : Temperature Profile Around the Arc Column in SF_6 Gas Flow, 2nd Int. Conf. on Gas Discharges (London), IEE Pub. **90** (1972), 305-307.
15) I. Miyachi, K. JayaRam and Y. Asai: Steady State and Post-Arc Spatial Temperature Distributions in MEVARC, 2nd Int. Conf. on Gas Discharges (London), IEE Pub. **90** (1972), 364-366.
16) T. Inaba, Y. Kito and I. Miyachi: Radial Distribution of Current Density and Temperature within a Heavy-Current Stabilized Arc Column in SF_6 Gas, Trans. IEE Japan **92-10** (1972), 47-A56, 457-467.
17) T. Inaba, Y. Kito and I. Miyachi: Voltage Gradient along Free-Burning Arc in SF_6 Gas, Trans. IEE Japan **93-2** (1973), 48-A11, 78-82.
18) I. Miyachi: Physical and Chemical Properties of Arcs and their Applications, JIEE Japan **93-5** (1973), 368-371.
19) T. Sakakibara, Y. Kito and I. Miyachi: Instantaneous Measurement of Spatial Temperature Distribution through Light Beams Deflection Method, J. Phys. E. **6-1** (1973) 40-42.
20) T. Inaba, Y. Kito and I. Miyachi: Pressure Dependent Characteristics of Wall-Stabilized SF_6 Gas Arc Columns, Trans. IEE Japan **93-4** (1973), 48-A21, 146-152.
21) I. Miyachi: Present Status of Research and Development on HVDC Circuit-Breakers, JIEE Japan **94-2** (1974), 105-108.
22) T. Sakakibara, Y. Kito and I. Miyachi: Voltage Gradient of Pressurized SF_6 Gas Arc in Very Low Current Range, 3rd Int. Conf. on Gas Discharges (London), IEE Pub. **118** (1974), 24-27.
23) I. Miyachi and H. Naganawa: Spiral Arc in SF_6 Facilitating DC Interruption, 3rd Int. Conf. on Gas Discharges (London), IEE Pub. **118** (1974), 521-524.
24) T. Sakakibara, Y. Kito and I. Miyachi: The Voltage Gradient of the Stabilized Arc Column in High Pressure SF_6 Gas, J. Phys. D. **7** (1974), 1975-1982.
25) T. Sakakibara, Y. Kito and I. Miyachi: Effect of Air Blast Velocity on Heat Transfer from Arc Column, Trans. IEE Japan **96-1**, (1976), 51-A3, 17-24.
26) Y. Kito, I. Miyachi and T. Adachi: Voltage Gradient of Wall-Stabilized Arc Column in Air, Trans. IEE Japan **96-6** (1976), 51-A37, 280-286.
27) Y. Kito, J. Miyachi and T. Sakakibara: Influence of Radiation Loss on the Stabilized Air Arc Characteristics, 4th Int. Conf. on Gas Discharges (Swansee), IEE Pub. **143** (1976), 1-4.
28) I. Miyachi and K. Horii: Lightning Discharge Triggered by Rocket and its Application, JIEE Japan **97-4** (1977), 274-277.
29) I. Miyachi: Present Status and Future Trend of Gas-Insulated Equipments, JIEE Japan **97-5** (1977), 327-329.
30) M. Nagata, Y. Yokoi and I. Miyachi: Electrical Breakdown Characteristics in High Temperature Gases, Trans. IEE Japan **97-5** (1977) 52-A29, 223-229.
31) H. Naganawa and I. Miyachi: Formation of Spiral Arc and its Dynamic Characteristics, Trans. IEE Japan **97-7** (1977), 52-B53, 433-439.
32) T. Matsumura, T. Sakakibara, Y. kito and I. Miyachi: Conductance Time-Constant of Transient Wall-Stabilized Air Arc Caused by Stepwise Current Injection, Trans. IEE Japan **97-10** (1977), 52-A66, 513-520.
33) T. Sakuda, Y. Kito and I. Miyachi: Enhancement of Electron Density in High Temperature Air Contaminated by Copper Vapor, Trans. IEE Japan **98-4** (1978), 53-A27, 209-214.
34) T. Mizuno, I. Miyachi and H. Naganawa: Arc Voltage Control by Modified Electrode Configuration in Spiral-Arc DC Interrupting Device, Trans. IEE Japan **98-9** (1978), 53-B91, 749-756.
35) H. Naganawa, H. Ohno and I. Miyachi: Expanding Speed of Spiral Arc and its Elect-

ric Field Intensity along the Column, Trans. IEE Japan **98-9** (1978), 53-B96, 789-796.
36) T. Matsumura, Y. Kito and I. Miyachi : Transient Aspects of Arc Conductance in Wall-Stabilized Air and SF_6 Disturbed by Step Changes in Current, 5 th Int. Conf. on Gas Discharges (Liverpool), IEE Pub. **165** (1978), 138-141.
37) M. Nagata, I. Miyachi and Y. Yokoi : Breakdown Characteristics of High Temperature Gases, 5th Int. Conf. on Gas Discharges (Liverpool), IEE Pub. **165** (1978), 316-319.